Electronic Structure of Host Lattices for Intercalation Compounds: SnS_2, $SnSe_2$, ZrS_2, and TaS_2

Anna Ibarz, Eliseo Ruiz, and Santiago Alvarez*

Departament de Química Inorgànica, Universitat de Barcelona, Diagonal 647, 08028 Barcelona, Spain

Received March 9, 1998

A theoretical study is presented on the electronic structure of some two-dimensional metal chalcogenides that are of great interest as host lattices for the intercalation of metallocenes. The periodic Hartree−Fock calculations with a posteriori correction for the correlation energy were carried out for the layer structures of SnS_2, $SnSe_2$, ZrS_2, and TaS_2. The band dispersion diagrams, density of states plots, and electron density maps are reported. The crystal structures were optimized, and the interlayer interaction energies and the energy gained upon reduction of the host lattices in the model ionic intercalation compound $Li(MX_2)_4$ were calculated. Comparison of the reduction energies with the oxidation energies of the metallocene molecules suggests that guest-to-host electron transfer is important in determining the stability of the intercalation compounds.

The layered metal chalcogenides MX_2 form an interesting family of materials, a fact that is related to the facility with which the successive layers can be separated and host molecules can be intercalated.[1,2] Among others, the intercalation of metallocenes and other sandwich complexes in metal chalcogenides has been largely studied since Dines first reported the intercalation of cobaltocene and chromocene[3] in a variety of MX_2 host lattices (M = Ti, Zr, Hf, Nb, Ta, Sn; X = S, Se). The host−guest interactions in the intercalation compounds are weak enough as to make the intercalation process reversible, but each host lattice shows some selectivity toward the intercalated species. The magnetic and electrical properties of the host lattice are often modified by the guest molecules, including a partial reduction of the host through electron transfer from the guest.[4−6] Although the crystal structures of the metal chalcogenides have long been known, those of the intercalation compounds have not been studied by single crystal X-ray diffraction, and partial information on the position of the guest molecule within the van der Waals gap has been obtained mainly from solid-state NMR spectroscopy.

The forces that hold the layers together in the pristine solid, as well as those that bond the host molecules to the guest layers, are weak ones: electrostatic, van der Waals or hydrogen bonds. Therefore, in order to tailor the properties of the intercalation compounds, it is important to understand their electronic structures and to better understand the fine details of such interactions and the factors that control them. The electronic structures of these intercalation compounds and a theoretical study of the associated processes in the host lattices, such as exfoliation or reduction, have not been reported so far. Furthermore, the properties relevant to the intercalation process have not been addressed by previous theoretical studies. Although one can find in the literature a variety of theoretical studies of the metal chalcogenides,[7,8] none has been carried out with the chemically oriented Hartree−Fock ab initio calculations. We have therefore undertaken a periodic ab initio study of the metal chalcogenides SnS_2, $SnSe_2$, ZrS_2, and TaS_2, carried out at the Hartree−Fock level with a posteriori correction for the correlation energy, as implemented in the CRYSTAL program.[9,10] With this methodology we studied the electronic structure of the host lattices, the interlayer cohesive energy, and the energy for the electron transfer associated with intercalation and compared the results with the oxidation energy for ferrocene, nickelocene, and cobaltocene. The electronic structure of the cobaltocene intercalation compounds in SnX_2 (X = S, Se), and a study of the host···guest interactions therein, will be reported elsewhere.[11]

Crystal Structure of SnS_2, $SnSe_2$, ZrS_2, and TaS_2

The metal chalcogenides MX_2 are layered compounds with strong M−X bonds within the layers and weak van

(1) O'Hare, D. In *Inorganic Materials;* 2nd ed.; Bruce, D. W., O'Hare, D., Eds.; John Wiley & Sons Ltd: New York, 1996; pp 171.
(2) O'Hare, D.; Evans, J. S. O. *Comments Inorg. Chem.* **1993**, *14*, 155.
(3) Dines, M. B. *Science* **1975**, *188*, 1210.
(4) Gamble, F. R.; Thompson, A. H. *Solid State Commun.* **1978**, *27*, 379.
(5) Wong, H.; Millet, R.; Evans, J. S. O.; Barlow, S.; O'Hare, D. *Chem. Mater.* **1995**, *7*, 210.
(6) Green, M. L. H.; Ng, D. K. P.; Wong, H. V. *J. Chem. Soc., Dalton Trans.* **1993**, 3213.
(7) Doni, E.; Girlanda, R. In *Electronic Structure and Electronic Transitions in Layered Materials;* Grasso, V., Ed.; D. Reidel: Dordrecht, 1986.
(8) Hess, A. C.; Clerc, D. G.; Poshusta, R. D. *J. Phys. Chem.* **1996**, *100*, 15735.
(9) Pisani, C.; Dovesi, R.; Roetti, C. *Hartree−Fock Ab-Initio Treatment of Crystalline Solids;* Springer Verlag: Berlin, 1988.
(10) Dovesi, R.; Saunders, V. R.; Roetti, C.; Causà, M.; Harrison, N. M.; Orlando, R.; Aprà, E., *CRYSTAL95*, Universitá di Torino, CCLRC Daresbury Laboratory, 1996.
(11) Ibarz, A.; Ruiz, E.; Alvarez, S. *J. Mater. Chem.* **1998**, *8*, 1893.

10.1021/cm980704w CCC: $15.00
Published on Web 09/03/1998

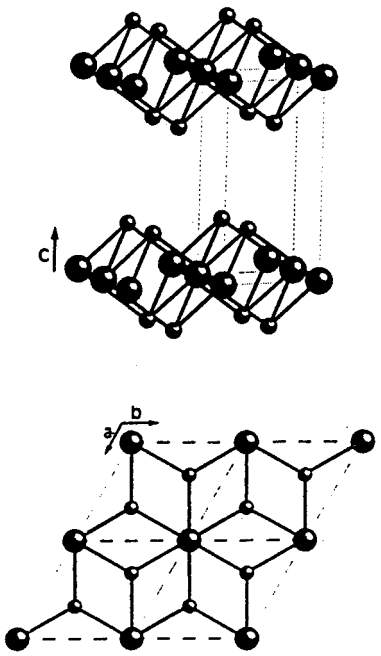

Figure 1. Structure of SnS_2 (above) and its projection along the *c* axis (below). Large circles represent the Sn atoms, small circles the S atoms.

der Waals interactions between the layers. The fact that the metal can be either in an octahedral or trigonal prismatic environment, together with the plasticity of the van der Waals interactions that allow different stacking patterns for the successive layers, gives rise to polymorphism in metal chalcogenides.[12,13] The structures studied here correspond to the CdI_2 type (Figure 1), in which there is only one MX_2 formula unit per unit cell. Each metal atom is surrounded by six anions with an approximately octahedral coordination sphere, and each anion is coordinated to three metal atoms with a trigonal pyramidal geometry. The neighboring layers are stacked in such a way that each metal atom is directly above another metal atom of the lower layer.

In the present studies we first optimized the crystal structure of the four solids at the Hartree−Fock (HF) level. Since the neglect of electron correlation by such a method is known to overestimate the nonbonded distances, we have introduced a posteriori a correlation energy correction according to the functional proposed by Perdew.[14,15] The results are shown in Table 1, together with the experimental data for comparison. The agreement between the calculated and experimental unit cell parameters is good at the HF level and very good with the correlation correction (HF+P91). Some discrepancies in the interatomic distances might be associated with the fact that the positional parameter *z* was kept fixed in the refinement of the crystal structures but has been optimized in our calculations.

Table 1. Structural Data Optimized for the MX_2 Solids at the Hartree−Fock Level (HF) and with a Posteriori Correction of the Correlation Energy (HF+P91)[a]

	HF	HF+P91	expl
	SnS_2		
a	3.720	3.653	3.620
c	6.000	5.845	5.850
z	0.2350	0.2350	0.250[b]
Sn−S	2.569	2.516	2.551
S···S	3.838	3.747	3.595
	$SnSe_2$		
a	3.804	3.794	3.794
c	6.362	6.212	6.132
z	0.2410	0.2410	0.250[b]
Sn−Se	2.679	2.563	2.675
Se···Se	3.961	3.893	3.770
	ZrS_2		
a	3.791	3.685	3.661
c	6.090	5.900	5.825
z	0.2350	0.2350	0.250[b]
Zr−S	2.615	2.540	2.568
S···S	3.900	3.893	3.601
	TaS_2		
a	3.695	3.490	3.360
c	5.980	5.845	5.900
z	0.2380	0.2475	0.250[b]
Ta−S	2.565	2.481	2.437
S···S	3.791	3.584	3.531

[a] Experimental data[16−19] is included for comparison. All values in Å, except *z* in fractional coordinates. [b] Not refined.

Nevertheless, the error is small for the M−X bond distances (smaller than 4% at the HF+P91 level) and not large for the nonbonded X···X distances (smaller than 7% at the HF+P91 level).

Electronic Structure of SnS_2, $SnSe_2$, ZrS_2, and TaS_2

Band dispersion diagrams and density of states plots have been obtained for the four solids at the optimized geometry. Those of the semiconducting solids SnS_2, $SnSe_2$, and ZrS_2 are presented in Figure 2. The electronic structure of TaS_2 will be discussed separately. The general aspects of the band structures of the three solids present some similarities: all of them show two low-lying occupied bands that correspond to the 3s and 3p orbitals of the chalcogen atoms and high-lying empty bands that correspond to the s and p valence orbitals of the metal atoms. The main differences correspond to the presence of the 4d bands above the Fermi level for ZrS_2. The splitting of the 4d bands in two subsets corresponding to the t_{2g} and e_g orbitals produced by the octahedral ligand environment can also be appreciated in Figure 2. These results are consistent with previous calculations using tight-binding,[20−23] density functional,[24−28] or hybrid methods.[27,29−31] For the semicon-

(12) Hulliger, F. In *Physics and Chemistry of Materials with Layer Structures;* Levy, F., Ed.; Reidel: Dordrecht, 1976.
(13) Whittingham, M. S. *Progr. Solid State Chem.* **1978**, *12*, 41.
(14) Perdew, J. P.; Yang, Y. W. *Phys. Rev. B* **1991**, *45*, 13244.
(15) Perdew, J. P.; Chevary, J. A.; Vosko, S. H.; Pederson, M. R.; Singh, D. J.; Fiolhais, C. *Phys. Rev. B* **1992**, *46*, 6671.
(16) Oftedal, I. *Norsk Geologisk Tidsskrift* **1926**, *9*, 225.
(17) Levy, F. *Structural Chemistry of Layered-Type Phases;* Reidel Publishing Co.: Dordrecht, The Netherlands, 1976.
(18) Conroy, L. E.; Park, K. C. *Inorg. Chem.* **1968**, *7*, 459.
(19) Jellinek, F. *J. Less-Common Met.* **1962**, *4*, 1962.
(20) Isomäki, H.; Boehm, J. V. *J. Phys. C: Solid State Phys.* **1980**, *13*, 3181.
(21) Murray, R. B.; Williams, R. H. *J. Phys. C: Solid State Phys.* **1973**, *6*, 3643.
(22) Roberston, J. *J. Phys. C: Solid State Phys.* **1979**, *12*, 4753.
(23) Bordas, J.; Robertson, J.; Jakobsson, A. *J. Phys. C: Solid State Phys.* **1978**, *11*, 2607.
(24) Fong, C. Y.; Cohen, M. L. *Phys. Rev. B* **1972**, *5*, 3095.
(25) Fong, C. Y.; Cohen, M. L. *J. Phys. C: Solid State Phys.* **1974**, *7*, 107.
(26) Müller, W.; Wiech, G.; Simunek, A. *Phys. Lett.* **1983**, *98A*, 66.
(27) Powell, M. J.; Marseglia, E. A.; Liang, W. Y. *J. Phys. C: Solid State Phys.* **1978**, *11*, 895.
(28) Schlüter, M.; Cohen, M. L. *Phys. Rev. B* **1976**, *14*, 424.

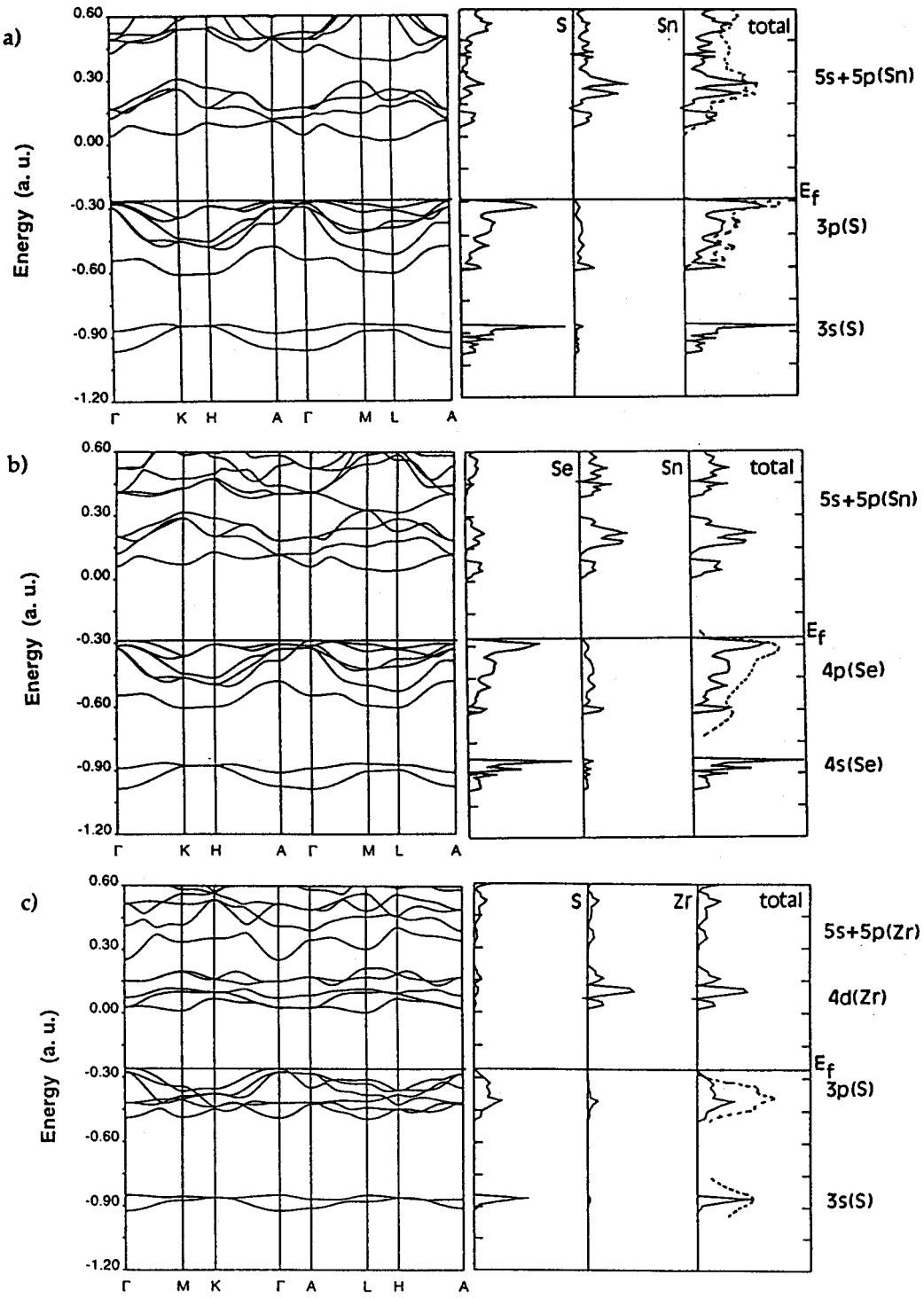

Figure 2. Band electronic structure, total density of states, and atomic projections for (a) SnS_2, (b) $SnSe_2$, and (c) ZrS_2. The XPS spectra[29−31] are schematically represented by the dashed lines together with the total DOS to facilitate comparison.

ducting compounds the total density of states is consistent with the previously reported XPS spectra.[32−34] The calculated bandwidths are consistent with, if somewhat larger than, those obtained from X-ray photoelectron,[32−37] X-ray absorption,[38] or Bremsstrahlung spectra.[39,40] It is well-known that the Hartree−Fock method overestimates the band gap;[9] hence, we make no comparison

(29) Isomäki, H. M.; Boehm, J. v. *Phys. Rev. B* **1982**, *26*, 5807.
(30) Isomäki, H.; Boehm, J. v. *Physica B C* **1980**, *99*, 255.
(31) Bullett, D. W. *J. Phys. C: Solid State Phys.* **1978**, *11*, 4501.
(32) Margaritondo, G.; Rowe, J. E.; Schluter, M.; Kasper, H. *Solid State Commun.* **1977**, *22*, 753.
(33) Williams, R. H.; Murray, R. B.; Govan, D. W.; Thomas, J. M.; Evans, E. L. *J. Phys. C: Solid State Phys.* **1973**, *6*, 3631.
(34) Wertheim, G. K.; DiSalvo, F. J.; Buchanan, D. N. E. *Solid State Commun.* **1973**, *13*, 1225.
(35) Berg, U.; Chasse, T. *Phys. Status Solidii* **1986**, *135*, 633.
(36) Margaritondo, G.; Rowe, J. E. *Phys. Rev. B* **1979**, *19*, 3266.
(37) Raisin, C.; Bertrand, Y. *J. Phys.C: Solid State Phys.* **1982**, *15*, 1805.
(38) Ohno, Y.; Hirama, K.; Nakai, S.; Sugiura, C.; Okada, S. *Phys. Rev. B* **1983**, *27*, 3811.
(39) Gao, Y.; Smandek, B.; Wagener, T. J.; Weaver, J. H.; Levy, F.; Margaritondo, G. *Phys. Rev. B* **1987**, *35*, 9357.

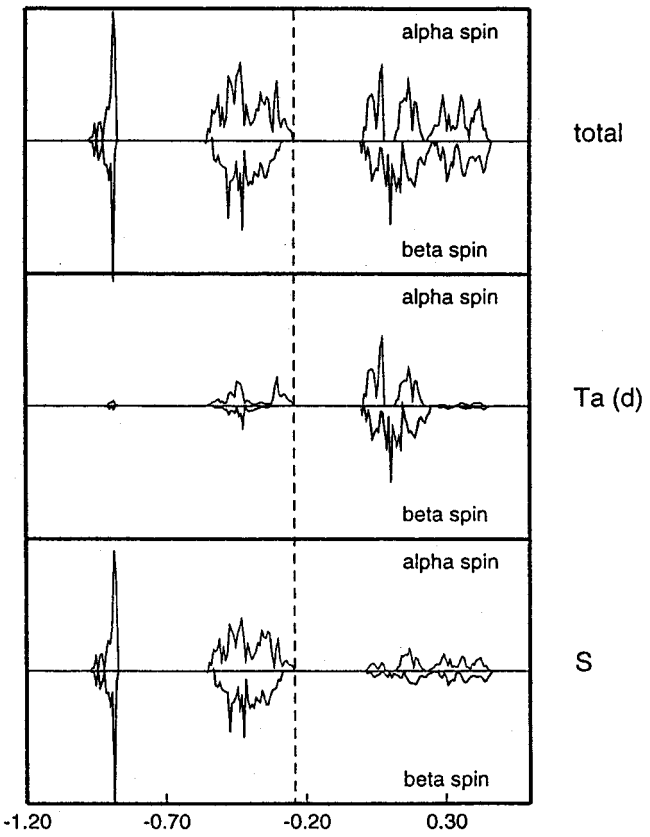

Figure 3. Total density of spin-up and spin-down states of TaS_2 and projections for the Ta and S atoms, obtained from unrestricted Hartree−Fock calculations at the optimized geometry. The dashed line indicates the Fermi level.

with the experimental optical properties reported for SnX_2.[41]

In the case of TaS_2, the d bands are partially occupied, consistent with its metallic character. In Figure 3 we present the density of states for the spin-up and spin-down states, as obtained from the unrestricted Hartree−Fock calculations with the optimized geometry. The unpaired electron corresponds to the spin-up d band below the Fermi level, whose spin-down counterpart is above the Fermi level. The analysis of the atomic orbital contributions shows that such a peak in the DOS corresponds to the d_{z^2} orbital of Ta, in agreement with the conclusions of photoemission spectra.[33,34,42,43]

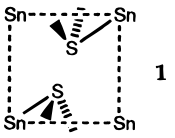

1

The electron density maps at the (110) plane are shown in Figure 4 for SnS_2, $SnSe_2$, and ZrS_2. The selected projection shows atoms of two layers, including one Sn−S bond of each layer. Also shown are the density differences between the crystal and the superposition of the spherical atomic densities for the same compounds. For TaS_2, we represent (Figure 5) the total electron density in the (110) plane, together with the difference between the spin-up and spin-down densities. The electron density maps show a deformation of the spherical symmetry in the direction of the M−X bonds, indicating some covalent character of the M−X bonding. The difference maps show along the M−X directions a larger density accumulation closer to the sulfide than to the selenide ions and closer to Zr than to the Sn atoms. Thus, the ionic character of the M−X bonds decreases in the order $ZrS_2 > SnS_2 > SnSe_2$, confirmed by the values of the net charges calculated through a Mulliken population analysis (Table 2). The electron donation from the chalcogenide to the transition metal ions goes mostly to the d orbitals for the transition metals Zr and Ta, but to the s and p orbitals in the case of Sn. The difference maps also show an electron density accumulation in the X···X interlayer direction, indicating some directionality of the van der Waals interactions, smaller for $SnSe_2$ than for SnS_2 and very small for ZrS_2. These electron density maps are consistent with those obtained with other computational methods.[25,28,44] In the case of TaS_2, the difference map

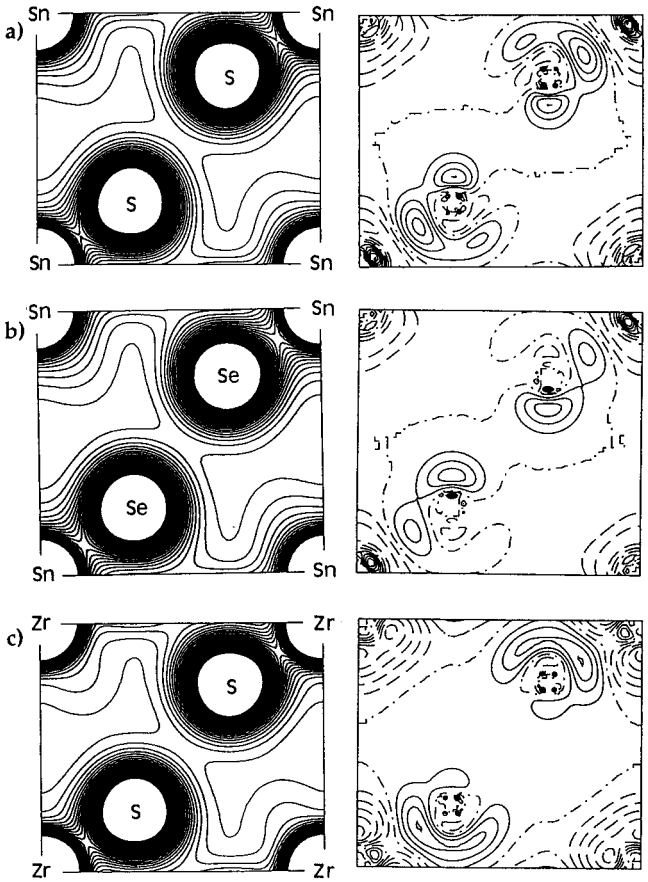

Figure 4. Total electron density (left) and difference between the total electron density and the superposition of the atomic spherical densities (right) in the (110) plane (see **1**) for (a) SnS_2, (b) $SnSe_2$, and (c) ZrS_2. Contours are shown at intervals of 0.005 $e^-/bohr^3$. In the difference plots, solid and dashed lines indicate an increase and a decrease of the electron density relative to the atomic superposition, respectively.

(40) Smandek, B.; Gao, Y.; Wagener, T. J.; Weaver, J. H.; Levy, F.; Margaritondo, G. *Phys. Rev. B* **1988**, *37*, 4196.
(41) Bertrand, Y.; Leveque, G.; Raisin, C.; Levy, F. *J. Phys. C: Solid State Commun.* **1979**, *12*, 2907.
(42) Dartigeas, K.; Gonbeau, D.; Pfister-Guillouzo, G. *J. Chem. Soc., Faraday Trans.* **1996**, *22*, 4561.
(43) Sherpherd, F. R.; Williams, P. M. *J. Phys. C: Solid State Phys.* **1974**, *7*, 4427.
(44) Wertheim, G. K.; DiSalvo, F. J.; Chiang, S. *Phys. Rev. B* **1976**, *13*, 5477.

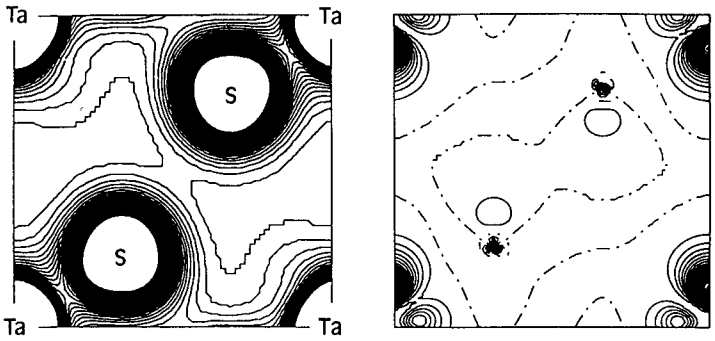

Figure 5. Total electron density (left) and difference between the spin-up and spin-down electron densities (right) in the (110) plane (see **1**) for TaS_2. Contours are shown at intervals of 0.005 e^-/bohr^3. In the difference plot, solid and dashed lines indicate a net positive and a net negative spin, respectively.

Table 2. Mulliken Population Analysis for the Optimized Structures

	SnS_2	$SnSe_2$	ZrS_2	TaS_2
net charge (M)	1.279	0.385	1.787	1.573
net charge (X)	−0.640	−0.192	−0.893	−0.787
orbital population (M)	5s 1.036	5s 1.166	5s 0.285	6s 0.387
	5p 1.357	5p 2.033	5p 0.222	6p 0.465
	5d 0.319	5d 0.390	4d 1.705	5d 2.575
orbital population (X)	3s 1.923	4s 1.902	3s 1.925	3s 1.921
	3p 4.659	4p 4.291	3p 4.923	3p 4.601
overlap population (M−X)	0.210	0.223	0.146	0.188

indicates that the unpaired electron is localized at the d_{z^2} orbital, as discussed above.

Interlayer Interaction

The possibility of theoretically estimating the energy of interaction between layers is highly interesting, both as a measure of the exfoliation capabilities of a solid and to allow one to calibrate its importance for the energetics of the intercalation processes. Such interaction energy was computed by calculating the energy of a solid at its optimized geometry (see above) and repeating the calculations with successive layers at a long distance (taking the translation vector along *c* equal to 12 Å). The van der Waals interactions between the layers are not well-handled by the Hartree−Fock method as found, for instance, by Hess et al.[8] for TiS_2. Accordingly, we will discuss only those energies calculated with the Perdew correction of the correlation energy (Table 3). Let us stress that the HF method with the a posteriori correction of the correlation energy yields a minimum at the interlayer separation corresponding to the optimized parameters (Table 1), close to the experimental values. Exfoliation of the solid requires approximately 1−2 kcal/mol according to our calculations, a value similar to that reported by Hess et al. for TiS_2. The small differences in the calculated energies suggest that the interaction is stronger for sulfides than for selenides and is in the sequence Zr > Ta > Sn. Comparison of the calculated interaction energies with the net charges on the X atom obtained from a Mulliken population analysis (Table 2) clearly indicates a correlation between the ionicity of the M−X bonds and the interaction energy (see Figure 6): the more ionic the M−X bond is, the stronger the interlayer interaction.

Since in some intercalation compounds there is a charge transfer from the guest to the host lattice, it is interesting to estimate the energetics of electron trapping by the metal chalcogenides. To that end, we

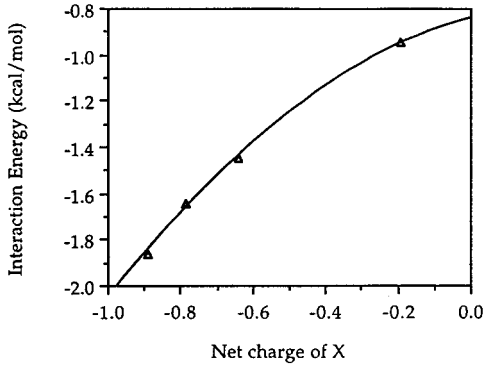

Figure 6. Calculated interaction energy between layers as a function of the net calculated charge on the X atoms in the metal chalcogenides MX_2 (energies in kcal/mol).

Table 3. Energy of Interaction between Layers (E_{int}) and Reduction Energies (E_{red}) Calculated at the HF+P91 Level (all Values in kcal/mol)

compd	E_{int}	E_{red}
SnS_2	−1.45	−147
$SnSe_2$	−0.95	−158
ZrS_2	−1.86	−217
1T-TaS_2	−1.64	−188
TiS_2	−1.30[8]	−170[8]

computed the energy of each compound with one Li atom intercalated in octahedral sites between the layers per four formula units of the host lattice. The geometries of the resulting $Li_{0.25}MX_2$ compounds were not optimized since Hess et al. had previously found that the interlayer distance is not altered upon lithium intercalation.[8] The difference between the energy of this intercalation compound and the sum of the energies of the two neutral sublattices is given in Table 3 for each of the studied chalcogenides. The resulting values are estimates of the energy gained by reducing the MX_2 lattice to $MX_2^{-0.25}$ combined with the electrostatic attraction between the Li^+ ion and the anionic sublattice. The electron transferred from the intercalated Li atom goes to the lowest unoccupied (or partially

Table 4. Relevant Bond Distances (Å) in the Neutral Metallocenes, MCp_2 (M = Fe, Co, Ni), and the Metallocenium Ions, MCp_2^+, as Obtained from B3LYP Calculations, and Experimental Data for the Neutral Molecules

	MCp_2		MCp_2^+
	calcd	expl[50−52]	calcd
	M = Fe		
M−C	2.101	2.064	2.141
C−C	1.435	1.440	1.431
C−H	1.080	1.104	1.080
	M = Co		
M−C	2.166	2.133	2.090
C−C	1.428	1.430	1.436
C−H	1.081	1.095	1.080
	M = Ni		
M−C	2.280	2.196	2.178
C−C	1.431	1.430	1.439
C−H	1.081	1.083	1.080

occupied, for M = Ta) band of the metal chalcogenide layers, i.e., the 5s(Sn) band or the nd(M) band for M = Ti, Zr, or Ta. The stronger nuclear attraction experienced by the d electrons results in a higher stabilization of the transition metal sulfides upon reduction compared to the Sn chalcogenides.

On the other hand, to obtain some estimate of the energetics of the charge transfer process that accompanies the intercalation of metallocenes in metal chalcogenides, we have calculated the energy required for the one-electron oxidation of neutral metallocenes MCp_2 (M = Fe, Co, Ni) at a similar level of theory (B3LYP). The structures of the neutral and oxidized forms of each metallocene were optimized (bond distances given in Table 4), obtaining a good agreement with the experimental data for the neutral species. The predicted shortening of the M−C distance upon oxidation of cobaltocene and nickelocene is in agreement with the antibonding character of the HOMO.[45] The calculated values of the oxidation energy are 145, 133, and 130 kcal/mol for ferrocene, nickelocene, and cobaltocene, respectively, in good agreement with the trends reported for the electrochemical reduction potentials[46] and the first ionization potentials determined from UV photoelectron spectra.[47] Comparison of these values with the energy gained upon reduction of the host lattice indicates that the energy needed to separate the layers of the host−lattice is provided by the electron transfer combined with the electrostatic host−guest interaction. The sum of the reduction energy of the host lattice, the oxidation energy of the metallocene, and the interlayer separation energy can give a rough estimate of the intercalation energy. Note that electron transfer to the host lattice is more favorable for cobaltocene and nickelocene than for ferrocene. These results are in excellent agreement with the different degrees of charge transfer found in the intercalation compounds that these lattices form with cobaltocene: for TaS_2 and ZrS_2, for which the energy needed to oxidize a cobaltocene molecule is more than compensated by the stabilization of the host upon reduction, a large degree of electron transfer has been proposed on the basis of the experimental data.[4,5] In contrast, for SnS_2, for which the electron transfer is less likely to be thermodynamically favored according to our estimates, the degree of charge transfer has been found to be of only a 25%.[48,49]

Concluding Remarks

A periodic ab initio study of some MX_2 layer compounds very well reproduces their crystal structures. The analysis of the electron density maps indicates that the ionic character of the M−X bonds decreases in the order $ZrS_2 > SnS_2 > SnSe_2$. Electron density accumulation in the X···X interlayer direction is observed, indicating some directionality of the van der Waals interactions, which is smaller for $SnSe_2$ than for SnS_2 and very small for ZrS_2.

Evaluation of the interlayer interaction energy indicates that exfoliation of the solid requires between 1 and 2 kcal/mol. Such interaction is stronger for sulfides than for selenides and varies with the nature of the metal atom according to the sequence Zr > Ta > Sn. In summary, the interlayer interaction seems to be stronger for those compounds with the more ionic M−X bond.

Calculations on the ionic intercalation compounds $Li_{0.25}MX_2$ allow us to estimate the energy gained upon reducing the MX_2 lattice to $MX_2^{-0.25}$, combined with the electrostatic attraction between the Li^+ ion and the resulting anionic sublattice. Comparison of those values with the calculated oxidation energies for three metallocene molecules (ferrocene, cobaltocene, and nickelocene) shows that charge transfer from the guest metallocene molecules to the host lattice provides a driving force for the intercalation process.

Appendix: Computational Details

The periodic Hartree−Fock calculations have been carried out with the CRYSTAL92 program,[53] using the tolerances described as 6 7 6 8 14 in ref 9 for the bands, DOS, electron density maps, and geometry optimization. The basis sets used were (6621/621/1) for S,[54] (63311/5311/41) for Se,[55] (633211/5321/521) for Zr,[55] and (633321/53311/531) for Sn.[56] For Ta we used the small-core pseudopotentials of Hay and Wadt.[57] In all cases the most diffuse exponents were optimized by minimizing the calculated energy at the experimental structure. For the calculation of the interaction and reduction energies, the tolerances described as 10 10 10 10 18 in ref 9 were used. The a posteriori correction of the electron correlation energy was made with the model of Perdew[14,15] implemented in the CRYSTAL95 program.[10] For the calculation of the reduction energy of TiS_2, the basis set and the geometry reported by Hess[8] were used. The interaction and reduction

(45) Albright, T. A.; Burdett, J. K.; Whangbo, M.-H. *Orbital Interactions in Chemistry;* John Wiley & Sons, Inc.: New York, 1985.
(46) Bard, A. J.; Garcia, E.; Kukharenko, S.; Strelets, V. V. *Inorg. Chem.* **1993**, *32*, 3528.
(47) Green, J. C. *Struct. Bonding (Berlin)* **1981**, *43*, 37.
(48) Formstone, C. A.; FitzGerald, E. T.; O'Hare, D.; Cox, P. A.; Kurmoo, M.; Hodby, J. W.; Lillicrap, D; Goss-Custard, M. *J. Chem. Soc., Chem. Commun.* **1990**, 501.
(49) Formstone, C. A.; Kurmoo, M.; FitzGerald, E. T.; Cox, P. A.; O'Hare, D. *J. Mater. Chem.* **1991**, *1*, 51.
(50) Haaland, A.; Nilsson, J. e. *Acta Chem. Scand.* **1968**, *22*, 2653.
(51) Hedberg, L.; Hedberg, K. *J. Chem. Phys.* **1970**, *53*, 1228.
(52) Hedberg, A. K.; Hedberg, L.; Hedberg, K. *J. Chem. Phys.* **1975**, *63*, 1262.
(53) Dovesi, R.; Roetti, R.; Saunders, V. R. *CRYSTAL92,* Universitá di Torino, SERC Daresbury Laboratory, 1992.
(54) Hehre, D. J.; Radom, L.; Schleyer, P. von R.; Pople, J. A. *Ab Initio Molecular Orbital Theory*; Wiley: New York, 1986.
(55) Schaefer, A.; Horn, H.; Ahlrichs, R. *J. Chem. Phys.* **1992**, *97*, 257.
(56) Godbout, N.; Salahub, D. R.; Andzelm, J.; Wimmer, E. *Can. J. Chem.* **1992**, *70*, 560.
(57) Hay, P. J.; Wadt, W. P. *J. Chem. Phys.* **1985**, *182*, 299.

energies were not calculated at the self-consistent DFT level, but a posteriori corrections to the HF results were applied, since it has been shown that similar results are obtained for solids with the two approaches.[58−60]

(58) Causà, M.; Zupan, A. *Chem. Phys. Letters* **1994**, *220*, 145.
(59) Zupan, A.; Causà, M. *Int. J. Quantum Chem.* **1995**, *56*, 337.
(60) Lichanot, A.; Merawa, M.; Causà, M. *Chem. Phys. Lett.* **1995**, *246*, 263.

Acknowledgment. This work has been funded by DGES through the research project PB95-0848-C02-01. The use of the computing resources at the Centre de Supercomputació de Catalunya (CESCA) was supported in part through a grant from the Fundació Catalana per a la Recerca and the Universitat de Barcelona.

CM980704W